J Mater Sci (2007) 42:2112–2120
DOI 10.1007/s10853-006-1190-5

# Electric properties of $Bi_4Ti_3O_{12}$(BIT)–$CaCu_3Ti_4O_{12}$ (CCTO) composite substrates for high dielectric constant devices

**A. G. Pinheiro · F. M. M. Pereira ·
M. R. P. Santos · H. H. B. Rocha ·
A. S. B. Sombra**

Received: 20 November 2005 / Accepted: 7 February 2006 / Published online: 15 December 2006

**Abstract** A study of the effect of the presence of BIT ($Bi_4Ti_3O_{12}$) in the dielectric and optical properties of the $CaCu_3Ti_4O_{12}$ (CCTO) is presented. The samples were prepared by the solid state procedure. Mechanical alloying followed by the solid state procedure has been used successfully to produce powders of $CaCu_3Ti_4O_{12}$ (CCTO) and BIT ($Bi_4Ti_3O_{12}$) to be used in the composites. We also look at the effect of the grain size of the BIT and CCTO in the final properties of the composite. The samples were studied using X-Ray diffraction, scanning electron microscopy (SEM), Raman and infrared spectroscopy. We also did a study of the dielectric function $K$ and dielectric loss of the samples.

The role played by the grain size of CCTO and BIT in the dielectric constant and structural properties of the substrates are discussed. For frequencies below 10 MHz the $K$ value presented by the CCTO100 sample is always higher than the $K$ value presented by the BIT100 sample. At 100 Hz the value of $K$ 1900 for the CCTO100 sample and 288 for the BIT100 sample. However for the composite sample one has an unexpected result. The dielectric constant is higher for all the frequencies under study. At 100 Hz the value of the $K$ is around 10.000 for the BIT10 sample. Which is more than one order bigger compared to the CCTO100 value for the same frequency. Therefore, these measurements confirm the potential use of such materials for small high dielectric planar devices. These composites are also attractive for capacitor applications and certainly for microelectronics, microwave devices (cell mobile phones for example), where the miniaturization of the devices is crucial.

## Introduction

High dielectric constants have been found in oxides of the type $CaCu_3Ti_4O_{12}$ [1–3] (CCTO) which shows a dielectric constant ($K$) at 1 KHz of about 10.000 that is nearly constant from room temperature to 300 °C. Oxides with the perovskite structure are well stabilized by their high dielectric constants ($K$) which lead these class of materials to a big number of technological applications [4]. However this behavior is generally associated to ferroelectric or relaxor properties. In these cases the highest value of $K$ is obtained during a phase transition (as a function of temperature) presented by the material.

The existence of a transition temperature is generally a problem when one is talking about applications of these materials. The reported results for CCTO shows that the $K$ is high but with small dependence on the temperature [3].

Such material is very promising for capacitor applications and certainly for microelectronics, microwave devices (cell mobile phones for example), where the miniaturization of the devices are crucial.

High $K$ ceramics make it possible to noticeably miniaturize passive microwave devices. Their size can typically be reduced in comparing with classical

---

A. G. Pinheiro · F. M. M. Pereira · M. R. P. Santos ·
H. H. B. Rocha · A. S. B. Sombra (✉)
Laboratório de Telecomunicações e Ciência e Engenharia
dos Materiais (LOCEM), Departamento de Física,
Universidade Federal do Ceará, Caixa Postal 6030,
Fortaleza, Ceará CEP 60455-760, Brasil
e-mail: sombra@fisica.ufc.br

resonators and filters by a factor of 1/*K* (relative dielectric constant)

In this paper we will study a composite bulk substrate with two different phases. The first ceramic will be the bismuth titanate $Bi_4Ti_3O_{12}$–BIT. It belongs to the family of ferroelectric materials with layered structures, which consists of three perovskite-like units ($Bi_2Ti_3O_{10}^{2-}$ ), sandwiched between bismuth oxide ($Bi_2O_2^{2+}$) layers. BIT single crystals has low dielectric constant ($K \sim 244$ at 1 KHz) and a very high Curie temperature ($T_C = 675$ °C), which makes it useful for various applications such as memory elements, optical displays, piezoelectric and piroelectric devices in a wide temperature range from 20 °C to 600 °C. Below room temperature it shows a orthorhombic Fmmm symmetry, which exhibits ferroelectric properties [1, 2].

BIT ceramics have been used in capacitors, transducers, sensors etc [3, 4]. The tunning of specific electric properties by compositional modification as well as the grain size effect could lead to modifications in the Curie temperature, conductivity, coercivity, compliance etc [5, 6].

Dielectric properties of BIT ceramics are highly dependent upon the grain size, phase content of the ceramic body and sintering temperature. Dielectric constant (*K*) of BIT ceramics sintered around 850 °C show values in the range of 235–250 in the frequency range of 100 Hz–100 KHz. The dielectric loss (*D*) shows a little increase with values around $1.6 \times 10^{-2}$ in this frequency range [7].

Therefore, ceramics of BIT can show a different dielectric behavior, depending on the particle size.

The second crystalline phase will be in the form of $CaCu_3Ti_4O_{12}$ (CCTO) [8–10] as discussed before. For this material, high dielectric constants have been found which shows a dielectric constant at 1 KHz of about 10.000 that is nearly constant from room temperature to 300 °C.

The structure of CCTO was previously determined from neutron powder diffraction data [10]. It belongs to space group Im3 (No. 204) [10]. Recently we propose the use of mechanical alloying to produce CCTO [11]. The mechanical alloying is proving to be a powerful technique to obtain any quantity of powder with controlled microstructure [12]. Recently a polymeric citrate precursor route was used to produce CCTO [13]. It was observed dielectric constant of 3.000 and loss around 0.3–0.35 at 1 KHz.

In this work we report the preparation of the ceramic of CCTO and BIT through the solid state route and use these materials together to prepare composite substrates. The produced samples were studied using X-ray diffraction, infrared and Raman Spectroscopy and Scanning Electron Microscopy techniques. The dielectric constant and loss were also studied in the range of 100 Hz–10 MHz. The production, and the study of the properties of the BIT–CCTO substrates is important in view of possible applications as bulk devices like microwave resonators and oscillators, thick and thin high *K* films.

## Experimental methods

### CCTO crystalline powder

Commercial oxides $Ca(OH)_2$ (Vetec, 97% with 3% of $CaCO_3$), titanium oxide ($TiO_2$) (Aldrich, 99%), CuO (Aldrich, 99%) were used in the CCTO preparation. The material was ground on a Fritsch Pulverisette 6 planetary mill with the proportionality of $Ca(OH)_2$-3CuO-4$TiO_2$ . Milling was performed in sealed stainless steel vials and balls under air. Mechanical alloying was performed for 30 min of milling. In this case the milling was used only to give a good homogeneity of the powder. However we already showed in the literature that for 100 h of milling the complete production of CCTO is possible [11]. The reaction occurring during milling can be summarized as:

$$Ca(OH)_2 + 3CuO + 4TiO_2 \xrightarrow{\text{IMPACTS}} CaCu_3Ti_4O_{12} + H_2O.$$

The compounds were also prepared by the conventional powder-sintering technique using the same starting materials. The ceramic was submitted to calcination and sintering (see Table 1) in air in the range of 900 °C to 1020 °C for 12 and 12 h respectively [14]. This ceramic is called CCTO100.

### BIT powder preparation

The used BIT powder was prepared by the solid sate reaction of $Bi_2O_3$ (Aldrich, 99%), and $TiO_2$ (Aldrich, 99%), at temperatures around 850 °C (See Table 1-BIT 100). The composites were prepared at different temperatures described in Table 1.1.

### Substrates and electrodes

The samples were prepared in a disk shape (with thickness around 1 mm). The electrodes are circular prepared using the screen printing technique

**Table 1** Sample compositions and experimental procedure

| Sample | Reaction | | Sinterization procedure |
|---|---|---|---|
| BIT100 | milled 40 min., calcinated 850 °C/1 h | BIT | 850 °C/1 h |
| BIT80 | 80% BIT + 20% CCTO | BIT$_{0.8}$ CCTO$_{0.2}$ | 930 °C/12 h |
| BIT50 | 50% BIT + 50% CCTO | BIT $_{0.5}$ CCTO $_{0.5}$ | 930 °C/12 h |
| BIT20 | 20% BIT + 80% CCTO | BIT$_{0.2}$ CCTO$_{0.8}$ | 1020 °C/12 h |
| BIT10 | 10% BIT + 90% CCTO | BIT $_{0.1}$ CCTO$_{0.9}$ | 1020 °C/12 h |
| CCTO100 | milled 30 h, calcinated 900 °C/12 h | CCTO | 1020 °C/12 h |

(diameter around 1 cm) using silver (Ag) (Joint Metal-PC200).

### X-ray diffraction

The X-ray diffraction (XRD) patterns were obtained at room temperature (300 K) by step scanning using powdered samples. We used 5 s for each step of counting time, with a Cu–Kα tube at 40 kV and 25 mA using the geometry of Bragg–Brentano.

### Scanning electron microscopy

The photomicrograph of the films of BIT100, BIT50 and CCTO100, were obtained on a Scanning Electron Microscope, Phillips XL-30, operating with bunches of primary electrons ranging from 12 to 20 keV, covered with a layer of carbon of 30 nm of thickness.

### Dielectric measurements

The Dielectric measurements were obtained from a HP 4291A Material Impedance Analyzer in conjunction with a HP 4194 Impedance Analyzer, which jointly cover the region of 100 Hz–1.8 GHz at room temperature (300 K).

### Infrared spectroscopy

The infrared spectra (IR) were measured using KBr pellets made from a mixture of powder for each sample. The pellet thickness varied from 0.5–0.6 mm. The IR spectra were measured from 400–1000 cm$^{-1}$ with a Nicolet 5ZPX FT-IR spectrometer

### Raman spectroscopy

Micro-Raman measurements were performed using a T64000 Jobin Yvon spectrometer equipped with an $N_2$-cooled charge coupled device (CCD) to detect the scattered light. The spectra were excited with an argon-ion laser (5145 Å). The spectrometer slits were set to give a spectral resolution always better than 2 cm$^{-1}$. The Raman scattering was measured in a back scattering geometry directly from the powder.

## Results and discussion

### X-ray diffraction

Figure 1 shows the X-ray diffraction (XRD) patterns of the samples BIT$_X$–CCTO$_{1-X}$ together with the XRD of the references (JCPDS), associated to CCTO(CCTO_REF) and BIT(BIT_REF), that were used in the sample preparation (as discussed before). In the same figure one starts with the XRD of sample BIT (BIT100) (see Table 1). For this sample one can easily identify all the peaks associated to BIT phase. For the sample BIT80 (BIT$_{0.8}$–CCTO$_{0.2}$ see Table 1) the presence of the CCTO phase is very weak. Weak peaks

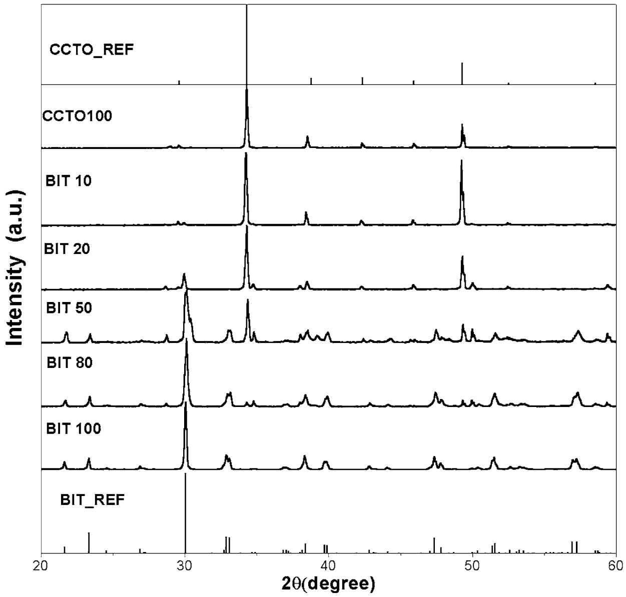

**Fig. 1** X-Ray diffraction of the samples in the series BIT–CCTO and reference samples (Joint Committee on Powder Diffraction Standards (JCPDS); International Center for Diffraction Data; 12 Camous Blvd.; Newton Square; Pennsylvania 19073–3723; USA; 19995—Pattern 93–1880 [BTO-reference], 75–1149 [CCTO-reference]

around 34.8° and 49.3°. Could be detected. For the sample BIT50 ($BIT_{0.5}$–$CCTO_{0.5}$) the presence of both phases is easily detected. The increase of the CCTO presence is quite clear. For the sample BIT10 ($BIT_{0.1}$–$CCTO_{0.9}$), the presence of BIT is quite weak. For the final sample in the series CCTO100, the CCTO presence is clear.

## Scanning electron microscopy

The particle morphology of the films was investigated by means of SEM. In Figs. 2, 3 and 4 for samples BIT100, BIT50 and CCTO100 respectively. For Figs. 2, 3 and 4 one has an amplification of ×5000, 5000 and 1000 respectively for the same samples. In Fig. 2 one has the SEM for the BIT100 substrate sintered at 850 °C for 1 h. One can notice that the sample exhibit long plates grains with good densification. In Fig. 3 one has the SEM associated to the composite BIT50 ($BIT_{0.5}$–$CCTO_{0.5}$). One can observe that the CCTO100 grains are much bigger compared to the BIT100 grains. The action of two grain sizes in the composite samples will lead to important consequences in the electrical properties that will be discussed later. In Fig. 4 (CCTO100 sample) one can notice the presence of the plates for the CCTO100 grains. These grains are bigger compared with the BIT100 grains. This is confirmed when one compares Figs. 2 and 4.

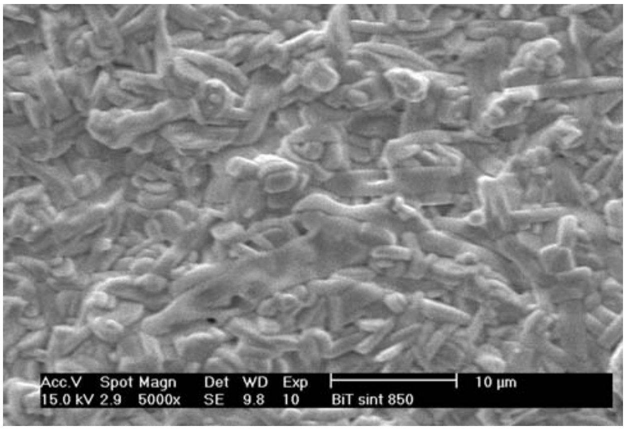

**Fig. 2** Scanning electron photomicrograph of BIT100 (5000×)

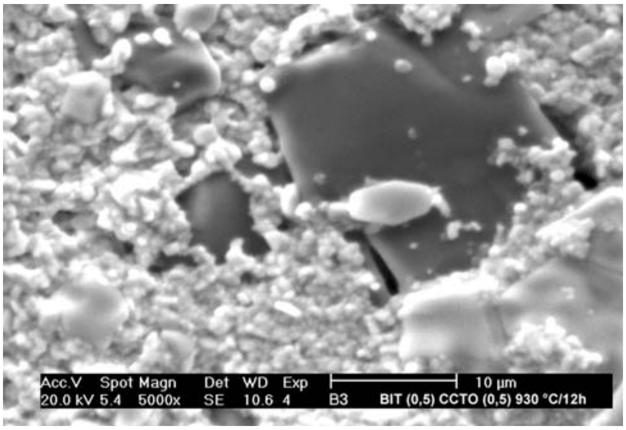

**Fig. 3** Scanning electron photomicrograph of the BIT50–CCTO50 (5000×)

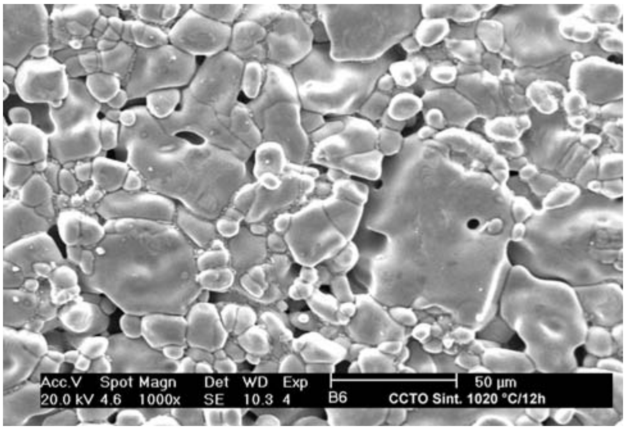

**Fig. 4** Scanning electron photomicrograph of the CCTO100 (1000×)

## Infrared spectroscopy

In Fig. 5 and Table 2 one has the infrared spectra of the samples in the series $BIT_X$–$CCTO_{1-X}$. The tetragonal BIT was characterized by the IR spectrum from octahedral TiO6 groups and the characteristic adsorption bands appeared at 830, 580 and 390 $cm^{-1}$

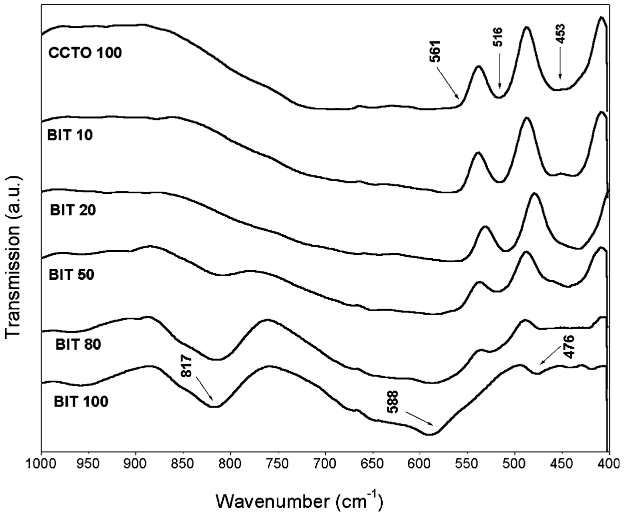

**Fig. 5** Infrared spectra of the substrates in the BIT–CCTO series

**Table 2** Infrared modes of the samples $BIT_X$–$CCTO_{1-X}$

| | Infrared modes ($cm^{-1}$) | | | | | | | |
|---|---|---|---|---|---|---|---|---|
| | BIT [45] | BIT 100 | BIT80 | BIT50 | BIT20 | BIT10 | CCTO100 | CCTO [46] |
| $v_1$(Ti–O–Ti) | | | 453 | 453 | 453 | 453 | | 441 |
| $v_1$(Ti–O) b | 390 | | | | | | | |
| | | 476 | | | | | | |
| $v_1$(Ti–O) | | | 516 | 516 | 516 | 516 | 516 | 516 |
| $v_1$(Ti–O) | | | 561 | 561 | 561 | 561 | 561 | 561 |
| $v_1$(Ti–O) s | 580 | 588 | | | | | | |
| $v_1$(Ti–O) s | 830 | 817 | 817 | 817 | | | | |

[15] (see Table 2 and Fig. 5). The bands above 405 $cm^{-1}$ was due to the Ti–O stretching vibration and the bands below 405 $cm^{-1}$ are attributed to Ti–O bending vibration [15]. Figure 5 shows the IR spectra of the BIT100 sample where the modes at 817 and 588 $cm^{-1}$ are identified. With the addition of 10% of the CCTO phases, new absorptions at 453, 516, 561 $cm^{-1}$ are present. These absorptions are associated to the CCTO phase. With the increase of the CCTO presence the modes at 588 and 817 $cm^{-1}$ associated to the BIT phase, are very weak. From the sample BIT20 all the detected modes are associated to the CCTO phase. One can notice that the CCTO phase present resonance absorptions at 561, 516 and 441 $cm^{-1}$. Several authors have assigned [9, 11, 12, 16] this region of absorptions with the titanium ion. These bands were associated to $\nu_{Ti\text{–}O}$ = 653–550 $cm^{-1}$ and $\nu_{Ti\text{–}O\text{–}Ti}$ = 495–436 $cm^{-1}$ (see Table 2)

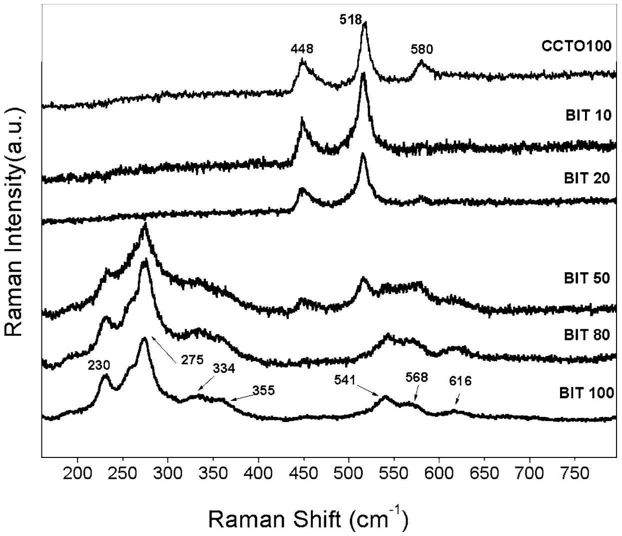

**Fig. 6** Raman spectra of the substrates in the BIT–CCTO series

In summary one can say that the main bands associated to BIT and CCTO were identified in the samples according with data from the literature.

## Raman spectroscopy

In Fig. 6 and Table 3 one has the Raman spectra of the samples of the complete series $BIT_X$–$CCTO_{1-X}$. The Raman spectra of the CCTO sample (CCTO100) has three main peaks at 448, 518 and 580 $cm^{-1}$ (see Fig. 6) in good agreement with values reported in the literature [17–19]. The Raman lines (Table 3) at 448 and 518 $cm^{-1}$ have $A_g$ symmetry ($TiO_6$ rotationlike). The peak at 580 $cm^{-1}$ is associated to a mode of Fg symmetry (O–Ti–O antistretching).

**Table 3** Raman modes of the samples $BIT_X$–$CCTO_{1-X}$

| Modes | Raman modes ($cm^{-1}$) | | | | | | | |
|---|---|---|---|---|---|---|---|---|
| | BIT [45] | BIT100 | BIT80 | BIT50 | BIT20 | BIT10 | CCTO100 | CCTO [46] |
| $B_{3g} + B_{2g}$ (O–Ti–O) | 227 | 230 | 230 | 230 | | | | |
| $B_{3g} + B_{2g}$ (O–Ti–O) | 268 | 275 | 275 | 275 | | | | |
| $A_{1g}$ (O–Ti–O) | 324 | 334 | | | | | | |
| $B_{1g}$(O–Ti–O) | 346 | 355 | | | | | | |
| $A_g$($TiO_6$) | | | 445 | 447 | 448 | 448 | 448 | 448 |
| $A_g$($TiO_6$) | | | 514 | 515 | 516 | 518 | 518 | 518 |
| $B_{3g} + B_{2g}$ (O–Ti–O) | 538 | 541 | | | | | | |
| $A_1g$ ($TiO_6$) | 558 | 568 | | | | | | |
| $A_{1g}$($TiO_6$) | 615 | 616 | | | | | | |
| $F_g$(O–Ti–O) | | | | 578 | | 580 | 580 | 580 |

In Fig. 6 one has the Raman spectra of the BIT sample. Modes at 616, 568, 334 and 355 cm$^{-1}$ could be assigned as the $A_{1g}$ and $B_{1g}$ modes, respectively (see Table 3); the 541,275 and 230 cm$^{-1}$ modes could be assigned as $B_{3g} + B_{2g}$ modes originating from the lifting of Eg degeneracy.

The Raman modes of the samples BIT and CCTO are in good agreement with the values reported in literature [11, 15, 16, 20], see Table 3.

For the composite film BIT80 the presence of CCTO was very weak through the Raman spectra. For the BIT50 sample, the mode at 520 cm$^{-1}$ associated to the CCTO phase is already present. For the BIT20 sample (see Fig. 6) the CCTO phase is dominant in the composite and the BIT phase is not detectable.

## Dielectric measurements

In Figs. 7 and 8 one has the dielectric constant measurements of all the samples of the series $BIT_X$–$CCTO_{1-X}$. One can notice that for all the samples the dielectric constant always decreases with the increasing of the frequency (see Fig. 7). For frequencies below 1 MHz the *K* value presented by the CCTO100 sample is always higher than the *K* value presented by the BIT100 sample. One can also notice that, the BIT10 sample ($BIT_{0.1}$–$CCTO_{0.9}$) present the highest dielectric constant up to 1 MHz of frequency. At 100 Hz the value of *K* 1900 for the CCTO100 sample and 288 for the BIT100 sample (see Table 4). However for the composite film one has an unexpected result. The dielectric constant is higher for all the frequencies under study. At 100 Hz the value of the *K* is around 10.000 for the BIT10 sample. Which is more than one order higher compared to the CCTO100 value for the same frequency (see Table 4). Our previous observations of the difference in the grain sizes of the two phases (Figs. 2–4) is suggesting that this difference in size for the composite is leading to a more effective densification of the sample, where little grains should more effectively fill empty spaces in the composite. This could lead to more effective interface effects that could lead to a higher dielectric constant to a specific composite concentration. This kind of effect was observed by our group in other composites of the series of ($BaTiO_3$) BTO–CCTO [21]. The other point is that for all the samples there is a general tendency to decrease of *D* (loss) with the increase of the frequency from 100 Hz to 1 MHz. This behavior is less accentuated for the BIT100 sample.

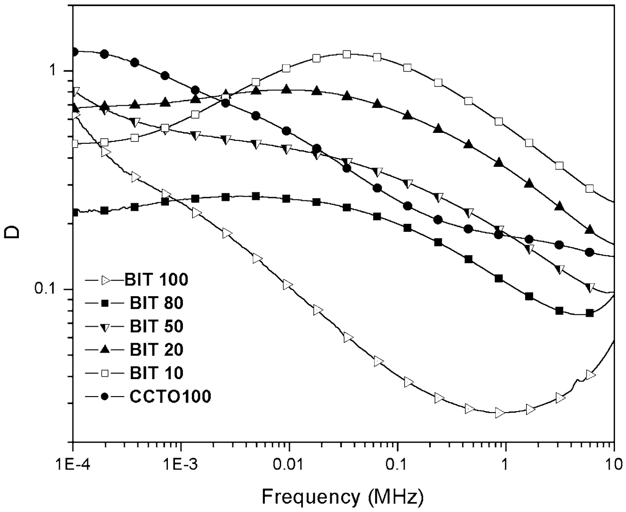

**Fig. 8** Dielectric loss (*D*) as a function of frequency of the samples in the BIT–CCTO series

**Table 4** Dielectric permittivity (*K*) and dielectric loss (*D*) of the samples $BIT_X$–$CCTO_{1-X}$

| Composite | *K D* (100 Hz) | *K D* (1 kHz) | *K D* (1 MHz) |
|---|---|---|---|
| BIT 100 | 288.1<br>0.62 | 217.4<br>0.24 | 159.0<br>0.027 |
| BIT 80 | 808.0<br>0.22 | 576.1<br>0.25 | 227.3<br>0.10 |
| BIT 50 | 1317.4<br>0.81 | 726.2<br>0.52 | 171.0<br>0.17 |
| BIT 20 | 5197.6<br>0.66 | 2097.9<br>0.72 | 170.4<br>0.35 |
| BIT 10 | 10908.1<br>0.46 | 5480.5<br>0.58 | 196.6<br>0.55 |
| CCTO 100 | 1909.2<br>1.22 | 648.3<br>0.87 | 164.8<br>0.17 |

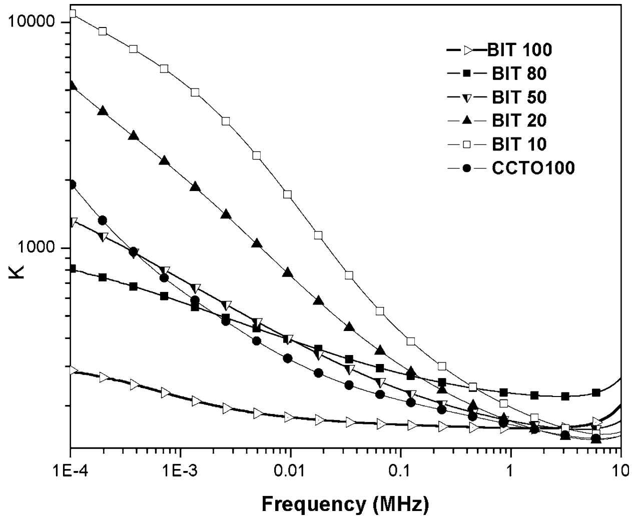

**Fig. 7** Dielectrc permittivity (*K*) as a function of frequency of the samples in the BIT–CCTO series

In Fig. 8 one has the dielectric loss for these samples. At 1 MHz the loss is lower for the BIT100 sample ($2 \times 10^{-2}$) and higher for the BIT10 sample (0.5).

This amazing behavior observed for the composite sample, where one has higher $K$ value compared to the pure states, is probably associated with the sizes of the grains in both phases and to the interface between these grains. We are now looking the presence of this effect in the microwave region as well.

The classic treatment applied for two or more phases present in a dielectric are associated to the dielectric mixing rules that fix a limit to the dielectric constant that can be achieved with the mixed phase. The empirical logarithmic rule for the dielectric constant $K$ and the dielectric constants ($K_I$) and relative volumes ($V_I$) of the individual phases ($I$ = 1 and 2 for BIT and CCTO) is given by [22]

$$\log K = \sum_I V_I \log K_I. \tag{1}$$

In Fig. 9 one has the plot of the dielectric constant ($K$) as a function of the substrate composition for the MF region and for several frequencies, based in Eq. 1.

The continuous line is associated to the value of $K$ obtained from Eq. 1, at 100 Hz.

The experimental points (for the frequencies 100 Hz, 1 kHz, 10 kHz, 100 kHz and 1 MHz) of the samples are also indicated in the figure. One can easily conclude that the increase of the BIT phase in the $BIT_X$–$CCTO_{1-X}$ composite is decreasing the $K$ of the substrate at 100 Hz of frequency. However for $x = 10\%$ the experimental value of the dielectric constant is much higher when compared to the expected value suggested by Eq. 1 ($K \sim 600$) at 100 Hz. This is an unexpected behavior. It means that the composite is not following the linear regime of the model. This behavior is present in all the studied frequencies (below 100 KHz)(see Fig. 9). In summary, three different composite substrates of BIT–CCTO were studied in the medium frequency range (MF) of the spectra.

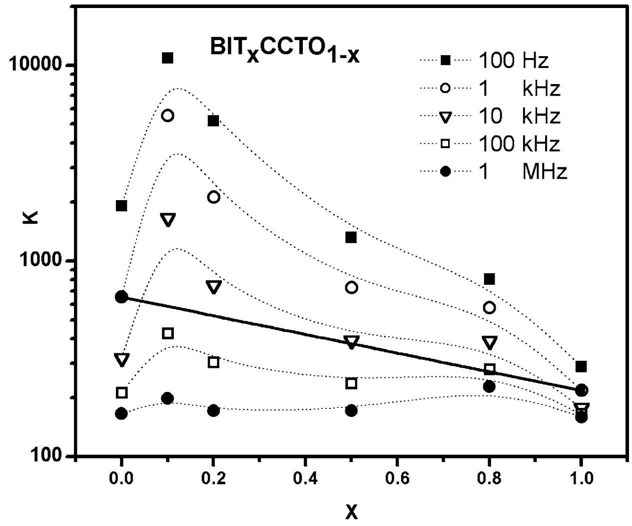

**Fig. 9** Dielectric permittivity for the Medium Frequency Range. Continuous line obtained from Eq. 1 ($f$ = 100 Hz). Experimental points extracted from Fig. 7

The dielectric permittivity $K$ of all the samples in the range of 100 Hz–1 MHz was studied. For all the samples there is a decrease of the $K$ value with frequency for this range of studied frequencies. The dielectric permittivity $K$ of the samples $BIT_X$–$CCTO_{1-X}$ were studied in the range of 100 Hz–10 MHz. One can observe that for the CCTO100 sample the dielectric constant $K$ is higher compared to the BIT100 sample for frequencies below 1 MHz. However for the samples where the BIT and CCTO form a composite ceramic, the dielectric constant is also decreasing with frequency.

One can say that the CCTO100 sample is presenting a higher value of $K$ at 100 Hz (1900) compared to the BIT100 sample (288). However the composite sample BIT10($BIT_{0.1}$–$CCTO_{0.9}$) is presenting a surprising effect, where the composite ceramic is not following the linear dielectric model with a $K$ value around 10.000 (see Fig. 9). This is a strong suggestion that a nonlinear mixing effect of the two phases is taking place.

## Conclusions

A study of the effect of the presence of BIT ($Bi_4Ti_3O_{12}$) in the dielectric and optical properties of the CCTO($CaCu_3Ti_4O_{12}$) was presented. The samples were prepared by the solid sate procedure. Mechanical alloying followed by the solid state procedure has been used successfully to produce powders of CCTO and BIT to be used in the composites. We also look at the effect of the grain size of the BIT and CCTO in the final properties of the composite. The samples were studied using X-Ray diffraction, scanning electron microscopy (SEM), Raman and infrared spectroscopy. We also did a study of the dielectric function $K$ and dielectric loss of the samples.

The X-ray diffraction (XRD) patterns of the samples $BIT_X$–$CCTO_{1-X}$ concludes that the BIT and CCTO phases are present in the composite samples.

The particle morphology of the films was investigated by means of SEM and suggest that the BIT sample exhibit long plates grains geometry with good densification. The CCTO sample present a plate geometry for the grains with bigger grains compared to the BIT sample. The action of two grain sizes in the composite samples will lead to important consequences in the electrical properties. The IR and Raman analysis shows the presence of the main Raman and IR modes associated to the BIT and CCTO phases reported in the literature [15, 16, 20, 21].

The dielectric constant ($K$) and loss ($D$) of the series $BIT_X$–$CCTO_{1-X}$ was studied in the range of 100 Hz–10 MHz. One can notice that for all the samples the dielectric constant always decrease with the increase of the frequency. For frequencies below 1 MHz the $K$ value presented by the CCTO100 sample is always higher than the $K$ value presented by the BIT100 sample. At 100 Hz the value of $K$ 1900 for the CCTO100 sample and 288 for the BIT100 sample. However for the composite samples one has an unexpected result. The dielectric constant is higher for all the frequencies under study. At 100 Hz the value of the $K$ is around 10.000 for the BIT10 sample. Which is more than one order bigger compared to the CCTO100 value for the same frequency which seems to be a nonlinear mixing effect of the two phases.

Our previous observations of the difference in the grain sizes of the two phases is suggesting that this difference in size for the composite is leading to a more effective densification of the sample, where little grains should more effectively fill empty spaces in the composite. This could lead to more effective interface effects that could lead to a higher dielectric constant to a specific composite concentration. The other point is that for all the samples, there is a tendency of decreasing the $D$ (loss) value with the increase of the frequency from 100 Hz to 1 MHz. This behavior is less accentuated for the BIT100 sample.

This amazing behavior observed for the composite sample is probably associated with the sizes of the grains in both phases and to the interface between these grains. We are now looking the presence of this effect in the microwave region as well.

Considering the classic treatment applied for two or more phases present in a dielectric and the empirical logarithmic rule for the dielectric constant $K$ and the dielectric constants $K_I$ of the individual phases one conclude that in the MF region of the spectra, the value of the dielectric constant is not in good agreement with the rule.

Looking now for high $K$ and low loss film, which is the best options for use in microwave devices like dielectric resonators, one has to find a balance between high dielectric constant and low loss. In a general view, the presence of the composite structure of BIT–CCTO is leading to a strong increase of the dielectric constant of the composite. We expect to find an equilibrium situation with the maximum for the dielectric constant and lower loss in the composite.

This strongly suggests that the composites BIT–CCTO are good candidates for applications where one are looking for high $K$ materials with low loss in radio-frequency range.

**Acknowledgements** This work was partly sponsored by FINEP, CNPq, FUNCAP and CAPES (Brazilian agencies).

## References

1. Aurivilius B (1949) Ark Kemi 1:499
2. Dorrain JF, Newnham RE, Smith DK (1971) Ferroelectrics 3:27
3. Takenaka T, Sakata K (1984) J Appl Phys 55:1092
4. Fouskova A, LE Cross (1970) J Appl Phys 41:2834
5. Alverez Fregoso O (1997) J Appl Phys 81:1378
6. Takenaka T, Sakata K (1981) Ferroelectrics 38:769
7. Kong LB, Ma J, Zhu W, OK Tan (2001) Mat Lett 51:108
8. Subramanian MA, Li D, Duran N, Reisner BA, Sleight AW (2000) J Sol State Chem 323:151
9. Ramirez AP, Subramanian MA, Gardel M, Blumberg G, Li D, Vogt T, Shapiro SM (2000) Solid State Comm 115:217
10. Subramanian MA, Sleight AW (2002) Solid State Sci 4:347
11. Almeida AFL, de Oliveira RS, Góes JC, Sasaki JM, Mendes Filho J, Sombra ASB (2002) Mat Sci Eng B 96:275
12. de Figueiredo RS, Messai A, Hernandes AC, Sombra ASB (1998) J Mat Sci Lett 17:449
13. Jha P, Arora P, Ganguli AK (2002) Mat Lett 4179:1–4
14. Koch M, Harris N, Maas R, Evans AGR, White NM, Brunnschweiler A (1997) Meas Sci. Technol 8:49
15. Dairong Chen, Xiuling Jiao (2001) Mater Res Bull 36:355–363
16. Music S, Gotic M, Ivanda M, Popovic S, Turkovic A, Trojko R, Sekulic A, Furic K (1997) Mat Sci Eng B 47:33
17. Ferrari V, Marioli D, Taroni A (1997) Meas Sci Technol 8:42
18. Morten B, De-Cicco G, Prudenziati M (1992) Sensors Actuators A31:153
19. Spitzer WG, miller RC, Kleinman DA, Howarth LG (1962) Phys Rev 126:5
20. Liua WL, Xia HR, Hand H, Wang XQ To appear in Journal of Crystal Growth
21. Almeida AFL, Fechine PBA, Góes JC, Valente MA, Miranda MAR, Sombra ASB (2004) Mater Sci Eng B 111(2–3):113–123A
22. Díaz-Güemes MI, Carreño TG, Serna CJ (1989) Spectrochimica Acta 45A:589
23. Lozinski A, Wang F, Uusimaki A, Leppavouri S (1997) Meas Sci Technol 8:33
24. Lucat C, Menil F, Von Der Muhll R (1997) Meas Sci Technol 8:38
25. White NM, Ko VTK (1993) Electronics Lett, August 1807
26. Chahal P, Tummala RR (1998) IEEE Trans Components, Packaging, Manuf Technol B21(2):184

27. Bhattacharya S, Tummala RR, Chahal P, White G (1997) International symposium on advanced packaging materials, p 68
28. Kinoshita K, Yamaji A (1976) J Appl Phys 47:371
29. Buessem WR, Cross LE, Goswami AK (1966) J Am Ceram Soc 49:33
30. Yen FS, Hsiang HI (1995) Jpn J Appl Phys 34:6149
31. Hsiang HI, Yen FS (1996) J Am Ceram Soc 79:1053
32. Arlt G, Hennings D, With GJ (1985) J Appl Phys 58:1619
33. Hsiang HI, Yen FS (1993) Jpn J Appl Phys 32:5029
34. Moulson AJ, Herbert JM (1990) Electroceramics. Chapman & Hall
35. Asiaie R, Zhu W, Akbar SA, Dutra PK (1996) Chem Matter 8:226
36. Preda L, Courselle L, Bandet J, Ianculescu A (2001) Thin Solid Films 389:43
37. Last JT (1957) Phys Review 105:6
38. Busca G, Uscaglia VB, Leoni M, Nanni P (1994) Chem Mater 6:955
39. Lee B, Zhang J (2001) Thin Solid Films 388:107
40. Wada M, Ohtuki T (1996) Phys B 219 and 220:635
41. Wang B, Zhang LD, Zhang L, Yan Y, Zhang SL (1999) Thin Solid Films 354:262
42. Cho W-S (1998) J Phys Chem Solids 59:659
43. Kolev N, Bontchev RP, Popov VN, Hadjiev VG, Litvinchuk AP, Iliev MN (2002) Physical Rev B 66:132102–1
44. Kreutz EW, Gottmann J, Mergens M, Klotzbucher T, Vosseler B (1999) Surface Coatings Technol 116:1219
45. He Q-y, X-g Tang, Zhang JX, I-m Wu (1999) Nanotructered mat.s, 11:287
46. Perry CH, Hall DH (1965) Physical Rev Lett 15:700
47. Ceramic Materials for Electronics (1991) R. C. Buchanan (ed.), Marcel Dekker Inc